URSI GASS 2021, Rome, Italy, 28 August - 4 September 2021

An Iterative Multifrequency Approach in L^p Spaces for Multiscaling Detection of Buried Objects

Andrea Randazzo* (1), Federico Capra(2), Claudio Estatico(3), Alessandro Fedeli(1),
Marco Salucci(2), Francesco Zardi(2), and Matteo Pastorino(1)
(1) Department of Electrical, Electronic, Telecommunications Engineering, and Naval Architecture, University of Genoa, Genoa, Italy; e-mail: {andrea.randazzo; alessandro.fedeli; matteo.pastorino}@unige.it
(2) ELEDIA Research Center (ELEDIA@UniTN – DISI), University of Trento, Trento, Italy;
e-mail: {federico.capra, marco.salucci, francesco.zardi}@unitn.it
(3) Department of Mathematics, University of Genoa, Genoa, Italy; e-mail: estatico@dima.unige.it

Abstract

The electromagnetic detection of buried objects is addressed in this paper, where a three-loop iterative imaging technique is proposed. A quantitative solution of the nonlinear inverse scattering problem is obtained by integrating a multiscaling strategy with a multifrequency inexact-Newton technique formulated in L^p spaces. Numerical results, where ground penetrating radar measurements have been simulated by a finite-difference time-domain method with various levels of data noise, demonstrate the advantages of the proposed strategy.

1 Introduction

One of the most promising fields of electromagnetic (EM) imaging is related to the detection of buried objects and structures. Recently, this kind of application has seen a great development as connected to ground penetrating radar (GPR), which is an unvaluable tool for civil and environmental engineering, as well as for archeology [1].
Although GPR subsurface prospection is known since decades, the interpretation of its measured data still represents an open research area [2], [3]. Indeed, the standard techniques applied in this framework are intrinsically qualitative, and most of the work is left to the users' expertise. However, there are plenty of interesting applications that could take advantage from a precise dielectric characterization of subsoil regions and the targets the soil conceals.
In general, the extraction of the dielectric properties of buried objects requires to solve a highly ill-posed nonlinear inverse scattering problem, which is made even more challenging due to the aspect-limited data which are normally available [4]. The exploitation of frequency diversity (i.e., multifrequency data) may mitigate some of these issues, but it should be combined with proper inversion algorithms.
For the quantitative multifrequency EM imaging of buried targets, good performances have been obtained with inexact-Newton schemes [5]. In this respect, it has been shown that defining inversion procedures outside the conventional Hilbertian spaces allows to improve the dielectric characterization of targets, avoiding the so-called over-smoothing regularization effects [6].
Further improvements in complex scenarios come from the adoption of multiscaling inversion approaches [7], which allow a suitable use of all the available data [8].
In this paper, the goal is to combine the benefits of both these inversion strategies, leading to a multifrequency multiscaling inexact-Newton algorithm formulated in L^p spaces for the effective detection of buried objects. This approach, whose implementation will be summarized in Section 2, has been validated by using data from EM simulations performed with a finite-difference time-domain solver. The main results are presented and discussed in Section 3. Section 4 draws conclusions.

2 Outline of the inverse scattering approach

Let us consider a configuration with two half-spaces with different dielectric properties, separated by a horizontal interface plane. The lowest one represents soil, which is characterized by relative dielectric permittivity ϵ_{rb} and electric conductivity σ_b. A two-dimensional imaging setup is assumed, with transverse-magnetic EM fields. In particular, the z component of the electric field scattered by buried targets at the frequency f is denoted as $E_f^{sc}(x,y)$. This quantity is measured in an observation domain $\mathcal{O}$ above the soil interface, i.e., for $(x,y) \in \mathcal{O}$. The unknown of the inverse problem is defined as the function $\psi(x,y) = [(\epsilon_r(x,y) - \epsilon_{rb})/c_\epsilon, (\sigma(x,y) - \sigma_b)/c_\sigma]^T$ in the buried investigation domain, i.e., $(x,y) \in \mathcal{D}$, where ϵ_r, σ are the unknown relative dielectric permittivity and electric conductivity of $\mathcal{D}$, and c_ϵ, c_σ are normalization coefficients. The multifrequency inverse problem can be summarized by the following system of equations:

$$\begin{bmatrix} \mathcal{A}_{f_1}(\psi)(x,y) \\ \mathcal{A}_{f_2}(\psi)(x,y) \\ \vdots \\ \mathcal{A}_{f_H}(\psi)(x,y) \end{bmatrix} = \begin{bmatrix} E_{f_1}^{sc}(x,y) \\ E_{f_2}^{sc}(x,y) \\ \vdots \\ E_{f_H}^{sc}(x,y) \end{bmatrix}, \qquad (x,y) \in \mathcal{O} \qquad (1)$$

where $\mathcal{A}_f$ is the nonlinear operator that describes the scattering phenomena at frequency f [5]. This problem, which can be compactly written as $\mathcal{A}(\psi) = E^{sc}$, is solved in the unknown ψ by adopting a multiscaling approach, i.e., with an iterative redefinition of the region of interest (RoI) within the investigation domain $\mathcal{D}$. For each scaling step $s = 1, \dots, S$, (1) is solved by considering a RoI $\mathcal{D}^{(s)}$, which is coincident to the whole $\mathcal{D}$ for $s = 1$ and is then adaptively refined in the subsequent steps, based on reconstruction results. For each step s, (1) is iteratively linearized around $\psi_i^{(s)}$, i.e., the current solution at the ith inexact-Newton iteration, obtaining a linear problem

$$\mathcal{A}'_{i,s}\delta_i^{(s)} = E^{sc} - \mathcal{A}\left(\psi_i^{(s)}\right) \quad (2)$$

where $\mathcal{A}'_{i,s}$ is the Fréchet derivative of $\mathcal{A}$ at $\psi_i^{(s)}$. This equation is solved with an L^p-space truncated Landweber regularization method [9], which represents the inner loop. Once $\delta_i^{(s)}$ is found, this term is applied as an increment to the actual solution, which is updated as $\psi_{i+1}^{(s)} = \psi_i^{(s)} + \delta_i^{(s)}$. Subsequently, a new RoI is defined by "filtering" and "clustering" the obtained dielectric profile [7], and the whole procedure is iterated until convergence is reached. This solution method is therefore composed by three nested loops: the outermost performs the iterative multiscaling approach; the intermediate one solves the multifrequency problem with a Newton-based procedure, and finally the innermost loop finds a regularized solution applying an L^p-space regularization.

3 Simulation results

The developed approach has been preliminarily evaluated with numerical simulations, comparing its performance against a previous code that does not integrate the multiscaling approach (i.e., a "bare" multifrequency inexact-Newton method in L^p spaces, MF-Lp [5]). The numerical tests have been performed by solving the forward electromagnetic problem with the *gprMax2D* finite-difference time-domain (FDTD) software [10], and corrupting the obtained total-field data (in the time domain) with a white Gaussian noise. Subsequently, total and incident fields in the frequency domain have been extracted through the Fourier transform.

The FDTD simulation domain is a square region with side length $L_{FDTD} = 6$ m, bounded by a perfectly matched layer (PML) and discretized into 750×750 square cells with side $l_{FDTD} = 0.008$ m. A time window of length $T_{FDTD} = 40$ ns has been simulated, adopting a time step equal to $\Delta t_{FDTD} = 18.9$ ps (i.e., 2120 FDTD iterations). The sources, modeled as axially directed current lines, have been excited with a Gaussian mono-cycle waveform with central frequency $f_0 = 300$ MHz. Electric field data at 200 MHz, 400 MHz, and 600 MHz have been used to perform the inversion process.

The measurement setup is multistatic and multiview [11]; it includes $V = 10$ different positions of the source and $M = V - 1$ measurement points for each view. Both sources and measurement points are located on a line at height $y^O = 0.1$ m from the soil interface, with horizontal coordinate ranging from $x_{min}^O = -0.564$ m to $x_{max}^O = 0.5$ m. The V probing positions are equally spaced, and while one of them is occupied by the source, in all the remaining ones the z component of the electric field is collected. The air-soil interface, located at $y = 0$, separates the upper half-space (modeled as air) from the lower half-space (modeled with relative dielectric permittivity $\epsilon_{rb} = 4$ and electric conductivity $\sigma_b = 10^{-3}$ S/m). A square investigation domain, with side length $L_{\mathcal{D}} = 0.8$ m and center at $(0, -0.4)$ m, is located inside the ground. Within $\mathcal{D}$, a dielectric cylinder with circular cross section of radius $r_{obj} = 0.08$ m is present. This target, whose barycenter is located at $(x_{obj}, y_{obj}) = (-0.16, -0.4)$ m, is characterized by $\epsilon_{obj} = 5.5$ and $\sigma_{obj} = 10^{-3}$ S/m (i.e., its contrast function with respect to the background is equal to $\tau = 1.5$).

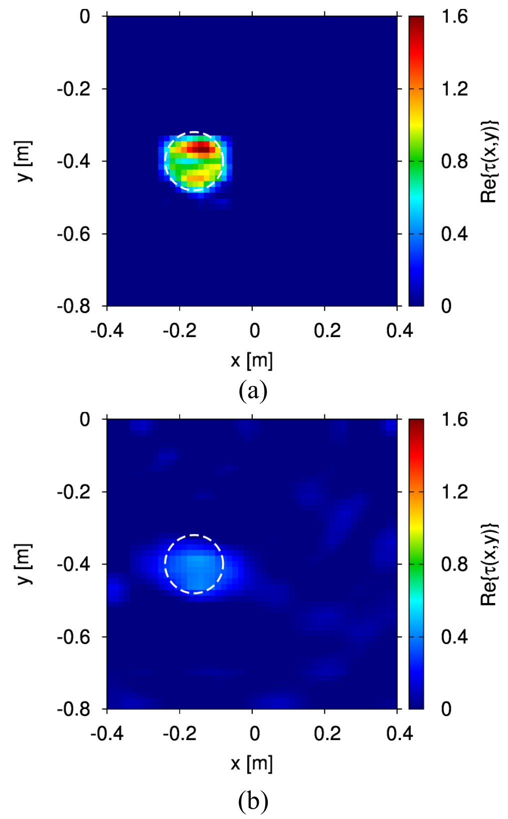

Figure 1. Reconstructed real part of the contrast function at 400 MHz with SNR = 30 dB. (a) Proposed approach and (b) MF-Lp reconstruction.

The proposed inverse solver has been run by considering a discretization with $N = 7 \times 7 = 49$ square cells, $S = 6$ maximum multiscaling steps (with zooming threshold equal to 0.2), and inexact-Newton/Landweber iterations $I = 100$ and $K = 1$, respectively. Conversely, the "bare" MF-Lp method, has been executed discretizing the investigation domain $\mathcal{D}$ with $N = 20 \times 20 = 400$ square cells, and with maximum number of iterations $I = 200$, $K = 10$. In both cases, the exponent value $p = 1.7$ has been adopted. The inversion methods have been assessed in the presence of both noiseless and noisy data, with signal-to-noise ratio (SNR) on the total time-domain electric field between 50 dB and 20 dB (corresponding to an average SNR on the scattered field in frequency domain equal to 31.43 dB and 1.43 dB, respectively).

The dielectric reconstructions obtained with SNR = 30 dB by the proposed approach and by the "bare" MF-Lp method are shown in Figure 1(a) and (b), respectively. Clearly, the proposed method outperforms the MF-Lp approach, and provides a more accurate localization and characterization of the buried object, yielding a reconstructed image which is almost free from background artefacts.
A quantitative comparison of the performances of these reconstruction methods has also been done by considering the relative reconstruction errors on the contrast function in the whole investigation domain (Ξ_{tot}), on the target only (Ξ_{int}), and on the background region (Ξ_{ext}). The values of these metrics, computed at the reference frequency of 400 MHz, are reported in Table 1 versus the level of data noise, for both the considered techniques. In all cases, reconstruction errors achieved by the developed technique are lower than those of the MF-Lp method.
Furthermore, the time required for to run the inversion codes, which is also reported in Table 1, evidences a significant computational saving obtained with the proposed inverse scattering approach.

Table 1. Reconstruction errors at 400 MHz versus the SNR, for the proposed approach and the standard MF-Lp method, with the corresponding computational times.

	SNR [dB]	Ξ_{tot}	Ξ_{int}	Ξ_{ext}	Time [s]
Proposed approach	∞	1.05×10^{-2}	2.26×10^{-1}	3.75×10^{-3}	171
	50	1.22×10^{-2}	2.48×10^{-1}	4.74×10^{-3}	171
	40	1.63×10^{-2}	3.01×10^{-1}	7.35×10^{-3}	194
	30	1.49×10^{-2}	2.63×10^{-1}	7.13×10^{-3}	177
	20	1.74×10^{-2}	2.94×10^{-1}	8.70×10^{-3}	235
MF-Lp	∞	6.27×10^{-2}	4.70×10^{-1}	4.98×10^{-2}	698
	50	6.31×10^{-2}	4.67×10^{-1}	5.03×10^{-2}	682
	40	6.53×10^{-2}	4.67×10^{-1}	5.26×10^{-2}	678
	30	7.98×10^{-2}	4.65×10^{-1}	6.78×10^{-2}	676
	20	1.44×10^{-1}	4.62×10^{-1}	1.34×10^{-1}	680

4 Conclusions

Buried objects detection by means of electromagnetic imaging represents a very challenging inverse problem, but the research on this topic is stimulated by the many potential applications of ground penetrating radar. In this paper, a quantitative inversion approach that integrates a multifrequency inexact-Newton method in L^p spaces with a multiscaling strategy has been presented. The developed numerical procedure has been preliminarily tested in a simulated environment, comparing the results with a "bare" application of the inexact-Newton approach. The comparison highlighted relevant benefits of the proposed method, in terms of both reconstruction quality and computational efficiency.

5 References

1. D. J. Daniels, *Ground penetrating radar*, 2nd ed. London: Institution of Electrical Engineers, 2004.

2. R. Persico, *Introduction to Ground Penetrating Radar: Inverse Scattering and Data Processing*. Hoboken, New Jersey: Wiley, 2014.

3. A. Benedetto and L. Pajewski, *Civil Engineering Applications of Ground Penetrating Radar*. Cham, Switzerland: Springer, 2015.

4. O. M. Bucci, L. Crocco, T. Isernia, and V. Pascazio, "Inverse scattering problems with multifrequency data: reconstruction capabilities and solution strategies," *IEEE Transactions on Geoscience and Remote Sensing*, **38**, 4, July 2000, pp. 1749–1756, doi: 10.1109/36.851974.

5. C. Estatico, A. Fedeli, M. Pastorino, and A. Randazzo, "A multifrequency inexact-Newton method in Lp Banach spaces for buried objects detection," *IEEE Transactions on Antennas and Propagation*, **63**, 9, September 2015, pp. 4198–4204, doi: 10.1109/TAP.2015.2446995.

6. I. Bisio, C. Estatico, A. Fedeli, F. Lavagetto, M. Pastorino, A. Randazzo, and A. Sciarrone, "Variable-exponent Lebesgue-space inversion for brain stroke microwave imaging," *IEEE Transactions on Microwave Theory and Techniques*, **68**, 5, May 2020, pp. 1882–1895, doi: 10.1109/TMTT.2019.2963870.

7. M. Salucci, L. Poli, N. Anselmi, and A. Massa, "Multifrequency Particle Swarm Optimization for Enhanced Multiresolution GPR Microwave Imaging," *IEEE Transactions on Geoscience and Remote Sensing*, **55**, 3, March 2017, pp. 1305–1317, doi: 10.1109/TGRS.2016.2622061.

8. M. Salucci, G. Oliveri, and A. Massa, "GPR Prospecting Through an Inverse-Scattering Frequency-Hopping Multifocusing Approach," *IEEE Transactions on Geoscience and Remote Sensing*, **53**, 12, December 2015, pp. 6573–6592, doi: 10.1109/TGRS.2015.2444391.

9. C. Estatico, A. Fedeli, M. Pastorino, and A. Randazzo, "Microwave imaging by means of Lebesgue-space inversion: An overview," *Electronics*, **8**, 9, September 2019, p. 945, doi: 10.3390/electronics8090945.

10. A. Giannopoulos, "Modelling ground penetrating radar by GprMax," *Construction and Building Materials*, **19**, 10, December 2005, pp. 755–762, doi: 10.1016/j.conbuildmat.2005.06.007.

11. M. Salucci, L. Poli, and A. Massa, "Advanced multi-frequency GPR data processing for non-linear deterministic imaging," *Signal Processing*, **132**, March 2017, pp. 306–318, doi: 10.1016/j.sigpro.2016.06.019.